CHIN.PHYS.LETT. Vol. 25, No. 10 (2008) 3811

An in-situ Observation on Initial Aggregation Process of Colloidal Particles near Three-Phase Contact Line of Air, Water and Vertical Substrate *

YAO Can(姚灿), WANG Yu-Ren(王育人)**, LAN Ding(蓝鼎), DUAN Li(段俐), KANG Qi(康琦)
National Microgravity Laboratory, Institute of Mechanics, Chinese Academy of Sciences, Beijing 100190

(Received 6 May 2008)

The self-assembling process near the three-phase contact line of air, water and vertical substrate is widely used to produce various kinds of nanostructured materials and devices. We perform an in-situ observation on the self-assembling process in the vicinity of the three phase contact line. Three kinds of aggregations, i.e. particle–particle aggregation, particle–chain aggregation and chain–chain aggregation, in the initial stage of vertical deposition process are revealed by our experiments. It is found that the particle–particle aggregation and the particle–chain aggregation can be qualitatively explained by the theory of the capillary immersion force and mirror image force, while the chain–chain aggregation leaves an opening question for the further studies. The present study may provide more deep insight into the self-assembling process of colloidal particles.

PACS: 82.70.Dd, 81.15.−z, 83.20.Bg

A three-phase contact line of air, water and solid substrate can be formed when a hydrophilic substrate is vertically put into a colloidal suspension. Water evaporation-driven capillary flow can force the colloidal particles in the suspension moving to the contact line and orderly aggregating in the meniscus region under the geometrical confinement of the contact line on the colloidal particles.[1] This self-assembling process has been widely used to fabricate various kinds of nanostructured materials, such as photonic crystals,[2−8] nano-fluidic sieves,[9] photonic glass,[10] nanotube surface arrays,[11] and patterning lines of colloidal particles.[12] Although the materials and application targets are different in those studies, the mechanisms involved in the processes are similar. The migration of a colloidal particle at the air–water interface is dominated by the lateral capillary force induced by the asymmetric distribution of contact line at the two sides of the colloidal particle.

Although many research works have been carried out to produce various kinds of materials based on the colloidal self-assembling process, the foundational studies of the colloidal particle interaction were mainly performed by Nagayama and co-workers. Kralchevsky and Nagayama[13] calculated the capillary forces between two particles partially immersing in a thin liquid film which is used to describe the two-dimensional self-assembling behaviour of colloidal spheres. In experiments, Denkov *et al.*[14] carried out an in-situ optical observation on the formation of close packed phase of micrometre-sized colloidal spheres under the acting of the capillary immersion force. Forces between two individual spheres[15,16] and between two cylinders[17] were measured in experiments to demonstrate the validity of the theoretical models and the calculations.

Recently, the vertical deposition (VD) method[18] was widely used for the fabrication of highly-ordered inverse-opal photonic band gap structures. In VD process, a clean glass slide was vertically put into the colloidal suspension. A three-phase contact line has been formed at the interface between the glass substrate and the colloidal suspension. With withdrawing of water on the glass substrate due to the water evaporation, a thin film containing highly-ordered colloidal spheres has been grown along the substrate. It was shown[6] that it is the evaporation-driven convective flow that pushes the colloidal particles moving towards the contact line. The evaporation rate, temperature and particle size are the main factors affecting this colloidal particle assembling process. In fact, research effort has never ceased to explore more details on the formation mechanism of the VD process, such as the role of the thickness transition[19] and the growth dynamics.[20] However, these investigations mainly focused on the large-scale behaviour of the self-assembling process, while the interactions among colloidal particle individuals were ignored commonly. On the other hand, theoretical studies on the inter-particle capillary force were reported in literature.[21−23] Different from the aggregation of colloidal particles on the water surface, introducing the glass substrate in VD process leads to the formation of the contact line and the interaction between the colloidal particle and the glass substrate. Analogically to the electrostatic interaction between an electric charge and a metallic plate, the capillary interaction between a floating sub-millimetre particle and a vertical wall can be seen as the interaction between a floating particle and its virtual mirror image particle. This interaction was referred to as mirror image force in literature. Therefore, the movement of colloidal particles on the contact line can be driven by both the lateral capillary

*Supported by the Knowledge Innovation Project of Chinese Academy of Sciences.
**Email: wangyr@imech.ac.cn

force and the mirror image force. Although a clear picture in physics can be derived from the theoretical research, more experimental studies on the problem are still needed to clarify the theoretical models.

In this study, we perform an in-situ observation on the self-assembling process of colloidal spheres in VD. We focus on studying the initial formation of the assembled particle line in the meniscus. This study may give more deep insight into the self-assembling dynamics and the capillary interaction between particles. Moreover, it is helpful to understand the nucleation process in growth of photonic crystal in VD.

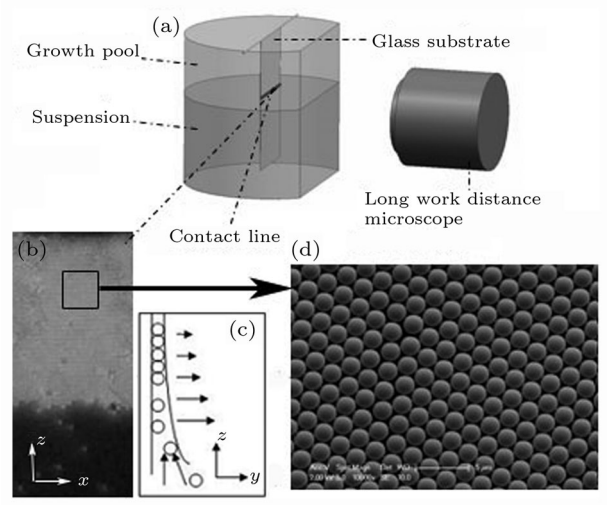

Fig. 1. (a) A schematic of the experimental setup. (b) A typical image of the as-grown colloidal film observed by the long working distance microscope. (c) A schematic of the particle assembling process in the meniscus region. (d) The SEM image showing the colloidal particle arrangement in the area marked in the square in (b). The diameter of PS particle is 2 μm.

Figure 1(a) shows a schematic diagram of the experimental setup. A cylindrical glass cell with a flat window was employed for the in-situ observation. The inside wall of the cell was chemically modified to be hydrophobic so that the light can not be curtained off before it enters the microscope lens. In experiment, a clean glass slide in dimensions $2.2 \times 1.0\,\mathrm{cm}^2$ was vertically mounted in the central part of the observation cell. The glass slides were dipped in the chrome acid solution for 12 h and cleaned several times in deionized water before used in experiment. Then, they were dried with high purity nitrogen gas. The whole cell was fixed in a temperature-constant chamber, which is not drawn in Fig. 1(a) for clarity. The chamber was kept at 55°C in experiment. We took 3 ml polystyrene (PS) suspension containing monodispersed PS spheres of 2 μm diameter at 1 vol%, put into the cell just at the beginning of the observation. A three-phase contact line of air, water and glass slide was formed as indicated by the straight solid line in Fig. 1(a). A long working distance microscope Questar QM100 with resolution of 1.5 μm and the shortest working distance of 15 cm was used for in-situ optical observation on the aggregation of colloidal particles. The images were recorded by the conventional videotape recorder.

The microscope was adjusted to focus on the area near the contact line. A typical image is shown in Fig. 1(b), which clearly indicates the interface between the grown film (the grey contrast) and the colloidal suspension (the black contrast). A schematic of the meniscus region is shown in Fig. 1(c). The highly-ordered arrangement of colloidal spheres in the grown film (in the solid square area) is illustrated in Fig. 1(d). We mainly observed the colloidal particle aggregation in the meniscus.

Before starting to discuss the experimental results, we summarize the theoretical results in the literature.[21−23] When a colloidal particle floats on the water surface, the particle gravity makes the deformation of water surface profile and subsequently changes the surface tension distribution around the particle. When two floating particles approach to each other at distance L, as shown in Fig. 2, the surface deformation on the two sides of the particle is different and asymmetric. The asymmetric surface profile around a particle will induce a lateral force to push the particle sticking together. It was demonstrated[13] that the capillary floating force F can be formulated as

$$F(L) \propto \left(R^6/\sigma\right) K_1(qL), \tag{1}$$

where σ is the surface tension, R is the particle radius, K_1 is the modified Bessel function, and $q = (\Delta\rho g/\sigma)^{1/2}$ is the reverse capillary length. On the other hand, there is another kind of lateral capillary force acting on the particle if the particle immersed in a thin liquid film.[13] The immersion force F^* can be formulated as

$$F^*(L) \propto \sigma R^2 K_1(qL). \tag{2}$$

In comparison of Eqs. (1) and (2), it can be found that the floating force decreases much faster than the immersion force with the decreasing particle radius. As reported in Ref. [13], the floating force is negligible if the particle radius is less than 5 μm. In contrast, the immersion force should be considered even if the particle radius is as small as 2 nm.

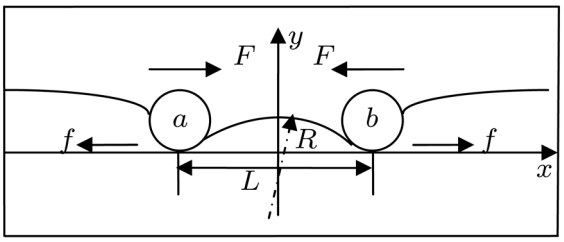

Fig. 2. A schematic of the capillary force acting on two colloidal particles floating on the water surface.

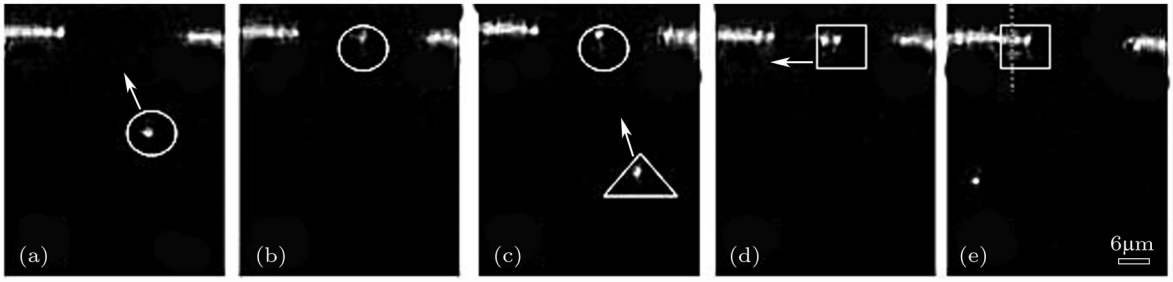

Fig. 3. A sequential images showing the particle–particle aggregation and the aggregation behaviour of their combination: (a) $t = 0$, (b) $t = 2\,\mathrm{s}$, (c) $t = 8\,\mathrm{s}$, (d) $t = 10\,\mathrm{s}$, (e) $t = 20\,\mathrm{s}$. Circles, triangles and squares in the images are used for guidance of eyes. The scale bar has the length of $6\,\mu\mathrm{m}$.

As mentioned above, the mirror image force which counts for the attraction between the particle and the vertical substrate must be considered in VD. The mirror image force has the same order in magnitude with the immersion force. It should be addressed that the mirror image force hinders the free movement of particle along the contact line and tends to pin the particle on the vertical substrate. Roughly speaking, the magnitude of the mirror image force acting on a chain is proportional to the number of the colloidal particles in the chain. In contrast, the immersion force acting on a chain is not larger than that acting on a pair of particles because only the two end particles in the chain have the asymmetric surface tension distribution, which origins from the immersion force. Therefore, it can be deduced that the movement of a single particle is easier than that of a long particle chain under the competing between immersion force and mirror image force.

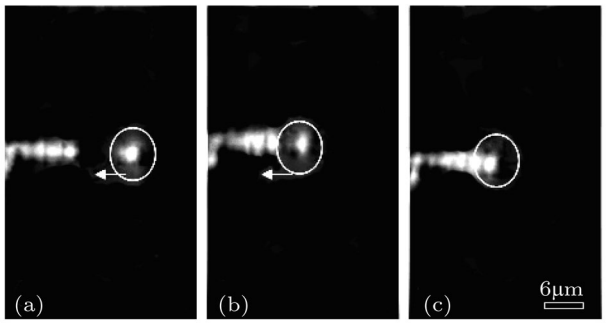

Fig. 4. A sequential of images illustrating the particle–chain aggregation behaviour: (a) $t = 0$, (b) $t = 1\,\mathrm{s}$, (c) $t = 2\,\mathrm{s}$. The scale bar in the image has the length of $6\,\mu\mathrm{m}$.

By our experiments, the particle aggregation behaviour can be divided into three classes, namely, particle–particle aggregation, particle–chain aggregation and chain–chain aggregation. The particle–particle aggregation counts for the aggregation process of two PS sphere individuals. The particle–chain aggregation describes the merging process of one PS sphere into a long PS particle chain, while the chain–chain aggregation is assigned to the merging process of two PS particle chains.

At the beginning of the experiment, the particles driven by evaporation arrive at the meniscus and they attract each other in a very fast speed and aggregate into short particle chains. The particle–particle aggregation into short chains occurs very fast in a few seconds. Figures 3(a)–3(d) show the merging of two particles into a short double-particle chain. A particle moves towards the contact line in Fig. 3(a) and stops at some positions shown in Fig. 3(b). Subsequently, another particle (triangle) occasionally moves to the vicinity of the first particle in the circle in Fig. 3(c). The two particles quickly combine into a double-particle chain shown in Fig. 3(d) when they approach within a short distance. This indicates that the immersion force applied to a single particle in the vicinity of other particles is strong enough to push the particle moving freely on the contact line, compared with the pinning effect of the image force. Figure 3(e) shows that the combined pair of particles merged into a neighbouring long chain. Comparison with the particle–particle aggregation, this process is much slower than the particle–particle aggregation. It can be interpreted by the enhancement of the image force with the increasing chain length, which is theoretically discussed in this study.

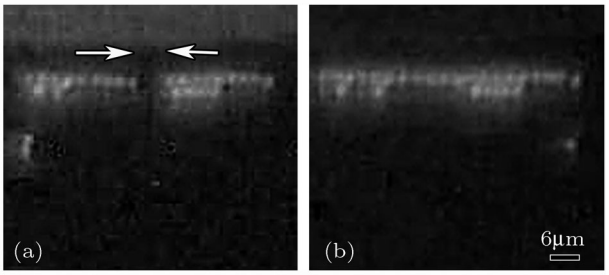

Fig. 5. Optical images showing the chain–chain aggregation. The scale bar in the image has the length of $6\,\mu\mathrm{m}$.

Figure 4 shows the process of one particle merging into a neighbouring chain. It can be seen that the particle moves across about $4D$ within 2 s, where D represents the diameter of the particle. It is indicated that the surface deformation-driven immersion force between two particles at distance of $4D$ is

strong enough to push the particle moving towards the chain. This experimental result is consistent with the theoretical prediction in Ref. [13]. Figure 5 shows the process of chain–chain aggregation. Two features deserved to be noted in the image. Firstly, the chain composing two particle rows can be clearly observed, while a large space is left between the two chains in the image. This means that the piling of the first particle row is not completed while the second row has been formed. This piling imperfection may form the initial defect nucleus in fabrication of ordered macroporous materials such as photonic crystal. The second feature is that the two long chains observed in the image still can merge together and form a longer chain, as shown in Fig. 5(b). This merging process of long chains, as is considered, cannot be completely assigned to the immersion force because the pinning effect of image force may be too large in this case.

In summary, we have performed an in-situ observation on the self-assembling process in VD. Three kinds of aggregation in the initial stage of VD process are revealed by our experiments. To out best knowledge, this is the first time for the report of in-situ observation on the initial stage of self-assembling process in VD. The particle–particle aggregation and the particle–chain aggregation can be qualitatively explained by the theory on the capillary immersion force and mirror image force, while the long chain–chain aggregation leaves an opening question for the further studies. It is believed that our studies may be helpful for deeply understanding the self-assembling process of several hundred nanometre-sized colloidal particles on the three phase contact line, which is widely used to produce various kinds of nanostructured materials and devices.

References

[1] Denkov N D, Velev O D, Kralchevsky P A, Ivanov I B, Yoshimura H and Nagayama K 1993 *Nature* **361** 26
[2] Velev O D, Jede T A, Lobo R F and Lenhoff A M 1997 *Nature* **389** 447
[3] Wijnhoven J E G J and Vos W L 1998 *Science* **281** 802
[4] Holland B T, Blanford C F and Stein A, 1998 *Science* **281** 538
[5] Velev O D, Tessier P M, Lenhoff A M and Kaler E W 1999 *Nature* **401** 548
[6] Dimitrov A S and Nagayama K 1996 *Langmuir* **12** 1303
[7] Ye Y H, LeBlanc F and Hache A and Truong W 2001 *Appl. Phys. Lett.* **78** 52
[8] Zhong Z G, Akira F and Osamu S 2002 *Chem. Mater.* **14** 760
[9] Zeng Y and Harrison D J 2007 *Anal. Chem.* **79** 2289
[10] Garcia P D, Sapienza R, Blanco A, Lopez C 2007 *Adv. Mater.* **19** 2597
[11] Tsukruk V V, Ko H and Peleshanko S 2004 *Phys. Rev. Lett.* **92** 065502
[12] Vyawahare S, Craig K M and Scherer A 2006 *Nano Lett.* **6** 271
[13] Kralchevsky P A and Nagayama K 1994 *Langmuir* **10** 23
[14] Denkov N D, Velev O D, Kralchevsky P A, Ivanov I B, Yoshimura H and Nagayama K 1992 *Langmuir* **8** 3183
[15] Dushkin C D, Kralchevsky P A, Yoshimura H and Nagayama K 1995 *Phys. Rev. Lett.* **75** 3454
[16] Dushkin C D, Kralchevsky P A, Paunov V N and Yoshimura H 1996 *Langmuir* **12** 641
[17] Velev O D, Denkov N D, Paunov V N, Kralchevsky P A and Nagayama K 1993 *Langmuir* **9** 3702
[18] Zheng Z Y, Liu X Y, Luo Y H, Cheng B Y, Zhang D Z, Meng Q B and Wang Y R 2007 *Appl. Phys. Lett.* **90** 051910
[19] Meng L L, Wei H, Nagel A, Wiley B J, Scriven L E and Norris D J 2006 *Nano Lett.* **6** 2249
[20] Lozano G and Miguez H 2007 *Langmuir* **23** 9933
[21] Paunov V N, Kralchevsky P A, Denkov N D, Ivanov L B and Nagayama K 1992 *Colloids and Surfaces* **67** 119
[22] Kralchevsky P A, Paunov V N, Denkov N D and Nagayama K 1994 *J. Colloid Interf. Sci.* **167** 47
[23] Kralchevsky P A, Paunov V N, Denkov N D and Nagayama K 1994 *J. Colloid Interf. Sci.* **167** 66